ARTICLE

Can Cyclopropyl-Terminated Self-Assembled Monolayers on Gold Be Used to Mimic the Surface of Polyethylene?

David Barriet, Pawilai Chinwangso, and T. Randall Lee*

Department of Chemistry and the Texas Center for Superconductivity, University of Houston, 4800 Calhoun Road, Houston, Texas 77204-5003

ABSTRACT This paper describes the formation of a new series of monolayer films generated by the self-assembly of ω-cyclopropylalkanethiols, CyPr$(CH_2)_n$SH ($n = 9-13$), onto the surface of gold. Procedures used to prepare the ω-cyclopropylalkanethiol adsorbates are also reported. Methyl-, vinyl-, and isopropyl-terminated self-assembled monolayers (SAMs) were also prepared and used as reference films to evaluate the structure and properties of the new cyclopropyl-terminated films. Ellipsometry and polarization modulation infrared reflection absorption spectroscopy (PM-IRRAS) were used to examine the structure of the SAMs. A small but systematically lower thickness of the new films compared to that of analogous methyl-terminated SAMs was observed. Also, the orientation of the ring with respect to the surface normal was observed to vary systematically with the number of methylene groups in the adsorbate backbone (i.e., odd vs even chain lengths). Measurements of wettability by contact angle goniometry also revealed a small but reproducible "odd−even" effect for all contacting liquids used, except hexadecane, which almost completely wet the surfaces ($\theta_a = 10-13°$). When compared to the wettability data obtained from methyl- and isopropyl-terminated SAMs, the wettability data obtained from the cyclopropyl-terminated SAMs suggest that these films offer an increased density of atomic contacts per unit area across the surface, and thus enhanced attractive interactions with contacting liquids. Comparison of the wettabilities of vinyl-terminated and cyclopropyl-terminated films is complicated by dipole−induced dipole interactions and/or $\pi-\pi$ interactions between the surfaces and the probe liquids. Furthermore, the significantly similar wettabilities of the cyclopropyl-terminated SAMs and the surface of polyethylene suggests that these SAMs (and perhaps other SAMs with judiciously designed tailgroups) can be used to mimic the interfacial properties of polymeric materials without complications arising from surface reconstruction.

KEYWORDS: polymer mimics • self-assembled monolayers • SAMs • gold • cyclopropyl tailgroups • wettability

INTRODUCTION

Both engineers and scientists have implemented a broad spectrum of techniques to evaluate the bulk and interfacial properties of polymers (1). The second endeavor has proven to be quite frustrating and constrained by the investigator's capacity to monitor and control the environmental conditions precisely at the interface to prevent the well-known phenomenon of reorganization of the surface (2). The continuing trend toward the nanoscale miniaturization of devices requires an increase in the surface-to-bulk ratio of materials. In theory, miniature devices that incorporate soft organic materials, such as polymers and lubricants, can access size regimes at the molecular (i.e., nanometer and subnanometer) level. Consequently, understanding the structure−property relationships at the interfaces of polymers at the nanoscale will be key to the next generation of nanodevices, including those relating to microelectromechanical systems (MEMs) (3−5), microfluidics (6, 7), dendrimeric drug delivery (8), and microelectronics (9, 10). Pursuing such applications for polymers requires appropriate model systems to investigate the interfacial chemistry of polymers in a systematic fashion (i.e., without shrouding by surface reconstruction). To this end, we have sought to use self-assembled monolayers (SAMs) to generate and study the chemistry of model polymer interfaces.

In the present study, we have chosen to model polyethylene, as it is the most important polymer in volume while being sufficiently simple in structure/composition that we can establish some firm grounds for further studies. Depending on the conditions adopted for the polymerization of ethylene, the degree of grafting and thus the proportion of methyl groups will vary greatly. As a consequence, the surface properties of the polymer will be greatly affected as demonstrated by the scatter in the reported contact angles for water on polyethylene that are found in the literature (11, 12). In this paper, we explore the relationship between the structure of a surface composed exclusively of methylene groups and its wettability (13). This issue is technologically relevant because a more profound understanding of the relationship between surface structure and wettability might lead to new and improved applications for polymers. We also wish to extract from our data some guidelines for engineers to find the proper conditions and/or formulation to afford desired interfacial properties.

Contact angle measurements are probably the oldest and the most widely used technique to characterize surfaces (14). Most often, however, contact angles are measured for an unknown surface and simply compared to charts of contact

* To whom correspondence should be addressed. E-mail: trlee@uh.edu.
Received for review February 23, 2010 and accepted March 04, 2010

DOI: 10.1021/am1001585

Published on Web 03/29/2010

angles obtained for a given polymer under various conditions without any true understanding of the structure/nature of the surface. Since the famed Young's equation (14), several elaborate theories have been put forward in efforts to correlate the contact angle measurements with the energy of interfaces. These efforts, however, have had limited success, especially in the case of inhomogeneously rough surfaces (15, 16). The difficulties in reconciling theories and experiments are probably associated with the fact that the theories try to connect a macroscopically observed phenomenon and differences in interfacial free energies for the three boundaries: solid/liquid, solid/gas, and liquid/gas (by definition, the contact angle should be measured at the three-phase point, so an approximation is made at the outset). These interfacial free energies are themselves dependent upon the nanoscale structure and composition of both the contacting liquid and the outermost few angstroms of the surface being evaluated.

Starting with the seminal paper by Nuzzo and Allara (17), self-assembled monolayers (SAMs) have proven themselves to be useful tools for designing and controlling interfaces at the nanometer scale. As alkanethiolates adsorb on the surface of Au(111), they form a monolayer of soft material whose structure and nature can be tailored through synthesis. When the quality of the gold used as substrate is acceptable (as judged by the size of the flat Au(111) terraces in AFM and/or the contact angle hysteresis), the SAM produced will present a smooth interface composed of a defined concentration of terminal groups (18). The structure of SAMs is determined by a balance of interactions between: (1) sulfur and gold, (2) the alkyl or aryl chains, and (3) terminal groups. Our interest in using SAMs to model/study polymer surfaces is driven by at least three factors: (1) the variety of polymer surfaces that can be investigated is limited only by the inventiveness in the design of adsorbates that can present the appropriate functional groups at the interface; (2) the literature presents a vast number of monolayers having widely differing terminal groups, which have been characterized using numerous surface-specific techniques, so the foundation for comparison is already laid; and (3) previous reports (19) have shown that SAMs derived from alkanethiols having at least ten carbon atoms (i.e., nine methylene groups) in the alkyl chain afford well-ordered monolayer films. In the work reported here, we designed all adsorbates accordingly. With well-packed films, we can expect to observe only a limited degree of reorganization during the time required for complete characterization of the system.

To model the surface of polyethylene, we chose to examine SAMs derived from the adsorption of cyclopropyl-terminated alkanethiols on gold. The choice of terminal cyclopropyl groups was driven by at least five factors. First, we anticipated that these adsorbates would form a densely packed surface composed exclusively of methylene groups. Second, the orientation of the cyclopropyl group (and thus the terminal methylene groups) could be systematically varied by changing the length of the methylene chain (odd vs even). Third, we chose to use the smallest ring possible because we hoped the size of the cyclopropyl group would not strongly affect the structure and packing of the monolayer film. This factor was a prerequisite to allow us to make unambiguous comparisons between the new surface and previously studied monolayers. Fourth, we wished to use this monolayer to shed new light on a statement that has been used for more than 40 years: "methylene groups are more wettable than methyl groups"; this concept was first introduced in the 1950s by Zisman and co-workers while comparing the surfaces of polyethylene, paraffins, and *n*-hexatriacontane (20, 21). It has been used quite extensively by surface scientists (including ourselves) (22−28) to rationalize the so-called "odd−even" effect (29, 30). The SAMs generated from alkanethiols having alternating alkyl chains lengths are generally attributed to the exposure of the higher energy methylene group adjacent to the terminal methyl in SAMs derived from alkanethiols having an odd number of carbon atoms (31−33). Variations in surface wettability (22, 23, 25, 28) and frictional properties (25, 26, 34) have been observed in various research groups. Even though a cyclopropyl methylene group might be different from an aliphatic methylene group (35), we felt this system would be valuable, given the minimal effect that such a small ring should have on the packing of the monolayer. Finally, another challenge was to address the sp^2 character of these methylene groups and its potential influence on the contact angles. To this end, we prepared vinyl-terminated SAMs and examined their structure and wettability. In addition, we used methyl-terminated SAMs as reference standards and isopropyl-terminated SAMs to make a direct parallel with the cyclopropyl group since this tailgroup contains two terminal methyl groups per adsorbate just as the cyclopropyl group contains two terminal methylene groups per adsorbate.

The structures of the cyclopropyl-terminated SAMs reported in this paper were characterized using ellipsometry (to evaluate the thickness of the films) and reflection absorption infrared spectroscopy (to evaluate the orientation and conformational order of the films). The interfacial wettabilities of the SAMs were characterized by contact angle goniometry using a combination of polar protic (water, formamide, and *N*-methylformamide), polar aprotic (*N*,*N*-dimethylformamide and acetonitrile), and apolar aprotic solvents (hexadecane and squalane). Methyl-terminated as well as vinyl- and isopropyl-terminated SAMs were used as the model references to evaluate the structure and properties of this new type of film.

EXPERIMENTAL SECTION

Materials. All contacting liquids were of the highest purity available from commercial suppliers and were used without purification. 11-Bromo-1-undecene was purchased from TCI America; all other ω-bromoalkenes were synthesized using conventional procedures involving the malonic ester synthesis, saponification, decarboxylation, and reduction followed by bromination. The ω-cyclopropylalkanethiols, $CyPr(CH_2)_nSH$ ($n = 9-13$), were prepared using the strategy outlined in Scheme 1. Because we used similar synthetic methods for most of these steps, we provide below the detailed procedures for all steps involved in the synthesis of $CyPr(CH_2)_{12}SH$ as a representative example. Nuclear magnetic resonance (NMR) data for ^1H and

Scheme 1. Synthesis of ω-Cyclopropylalkanethiols, $CyPr(CH_2)_nSH$ ($n = 9-13$)

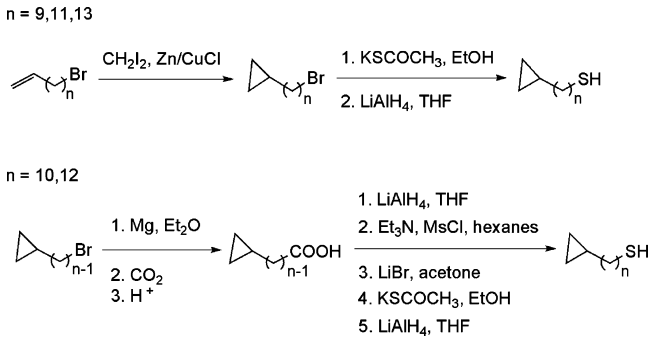

Scheme 2. Synthesis of ω-Alkenyl Disulfides

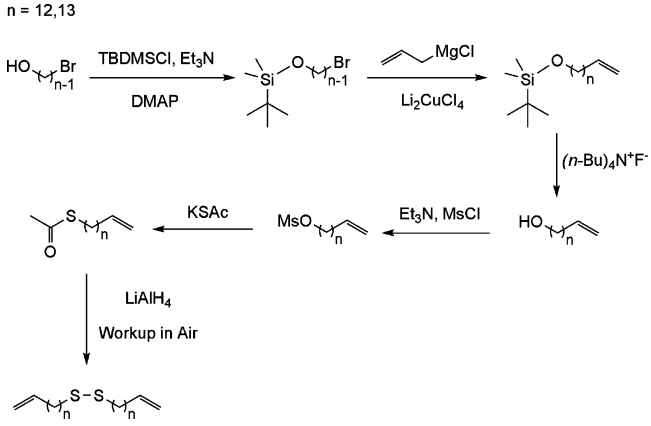

Scheme 3. Synthesis of ω-Isopropylalkanethiols

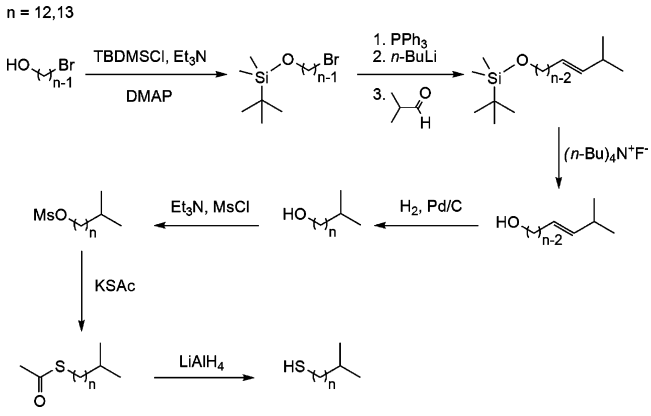

^{13}C nuclei of all ω-cyclopropylalkanethiols are reported. The actual NMR spectra for these final products are also provided as Supporting Information. Similarly, we describe the synthesis of ω-alkenyl disulfides and ω-isopropylalkanethiols (Schemes 2 and 3, respectively).

Synthesis of 12-Cyclopropyldodecanethiol. As shown in Scheme 1, the preparation of 12-cyclopropyldodecanethiol ($n = 12$) begins with the synthesis of 11-bromoundecylcyclopropane (36). Aliquots of anhydrous copper(I) chloride (9.86 g, 99.5 mmol) and zinc dust (6.51 g, 99.5 mmol) in 40 mL of diethyl ether were stirred and heated to reflux for 30 min under argon. Neat 11-bromo-1-undecene (10 g, 38 mmol) was added to the complex followed by methylene iodide (0.90 mL, 50 mmol), and the mixture was maintained at reflux for 40 h under argon. The mixture turned dark purple, indicating the formation of colloidal copper. The ether phase was poured onto a mixture of ice and 1 N HCl. The resulting ether phase was washed with brine (100 mL), dried over anhydrous $MgSO_4$, filtered, and concentrated to dryness. The crude product was composed of an estimated 60% of the desired cyclopropyl derivative and 40% olefinic starting material according to analysis by ^1H NMR spectroscopy. Attempts to recover the starting material by column chromatography on silica gel were essentially unsuccessful. Attempts to repeat the reaction using the crude product as the starting material brought limited improvements to the overall yield. The reddish crude product was diluted with dichloromethane (100 mL), and ozone was bubbled through the solution for 10 min at 0 °C. The solution was purged with argon, then dimethyl sulfide (8.48 mL, 115 mmol) was added to the cooled solution, which was stirred overnight at room temperature. The dichloromethane was evaporated, and the residue was purified by column chromatography on silica gel (hexanes, $R_f = 0.75$) to afford 5.77 g of 11-bromoundecylcyclopropane (55%) as a colorless liquid. ^1H NMR (300 MHz, $CDCl_3$): δ 3.42 (t, $J = 7.2$ Hz, 2 H), 1.86 (m, 2 H), 1.27 (bm, 18 H), 0.65 (m, 1 H), 0.38 (m, 2 H), −0.01 (m, 2 H).

12-Cyclopropyldodecanoic Acid. A pear-shaped 100 mL Schlenk flask loaded with magnesium turnings (0.794 g, 32.7 mmol) was flame-dried under vacuum. THF (5 mL) and a few crystals of sublimed iodine were introduced under a stream of argon. An aliquot of 11-bromoundecylcyclopropane (3.0 g, 11 mmol) diluted in 20 mL of dry THF was then added dropwise until a greenish color was observed; the addition rate was adjusted so as to maintain a gentle reflux. After completion of the addition, the mixture was stirred for an additional 30 min. The resulting Grignard reagent was quickly transferred under argon onto a large excess of dry ice (CO_2; 4.8 g, 0.11 mol). The mixture was left to warm for 30 min at room temperature. The reaction was carefully quenched using water (20 mL) and then diluted HCl (40 mL). The aqueous layer was separated from the organic layer and extracted with diethyl ether (3 × 30 mL). The combined organic layers were washed with brine (100 mL), dried over anhydrous $MgSO_4$, filtered, and concentrated to dryness. The crude product was purified by column chromatography on silica gel (20% diethyl ether/hexanes, $R_f = 0.36$) to afford 1.50 g of 12-cyclopropyldodecanoic acid (57%) as a white solid. ^1H NMR (300 MHz, $CDCl_3$): δ 2.35 (t, $J = 7.8$ Hz, 2 H), 1.62 (m, 2 H), 1.26 (bm, 18 H), 0.64 (m, 1 H), 0.37 (m, 2 H), −0.01 (m, 2 H).

12-Cyclopropyldodecanol. An aliquot of 12-cyclopropyldodecanoic acid (1.50 g, 6.25 mmol) diluted in 20 mL of dry THF was carefully added to a suspension of lithium aluminum hydride (0.474 g, 18.8 mmol) in 20 mL of dry THF cooled by an ice bath. The reaction mixture was refluxed overnight under argon. The reaction mixture was cooled to 0 °C and then quenched with a few milliliters of ethanol followed by acidification to pH ~1 using dilute HCl. The mixture was left stirring until the precipitate was completely dissolved. The aqueous layer was extracted with hexanes (3 × 20 mL). The combined organic layers were washed with brine (100 mL), dried over anhydrous $MgSO_4$, filtered, and concentrated to dryness. The solid residue was dissolved in a minimum amount of hexanes and purified by column chromatography on silica gel (20% diethyl ether/hexanes, $R_f = 0.17$) to afford 1.21 g of 12-cyclopropyldodecanol (85%) as a white solid. ^1H NMR (300 MHz, $CDCl_3$): δ 3.64 (t, $J = 7.5$ Hz, 2 H), 1.56 (m, 2 H), 1.26 (bm, 20 H), 0.63 (m, 1 H), 0.38 (m, 2 H), 0.00 (m, 2 H).

12-Cyclopropyldodecylmethanesulfonate. To an aliquot of 12-cyclopropyldodecanol (1.0 g, 4.4 mmol) diluted in 50 mL of hexanes was slowly added an aliquot (0.41 mL, 5.3 mmol) of triethylamine. The reaction mixture was left stirring at room temperature for 30 min. The solution was cooled in an ice bath, and then an aliquot (3.10 mL, 22.1 mmol) of methanesulfonyl chloride was added dropwise. The reaction was stirred for 4 h at room temperature to ensure completion. Excess methanesulfonyl chloride was destroyed using a small aliquot of water.

The precipitate was dissolved in 100 mL of water. The organic layer was separated, and the aqueous layer was extracted with diethyl ether (3 × 50 mL). The combined organic layers were washed with dilute HCl (100 mL), saturated aqueous $NaHCO_3$ (50 mL), and brine (100 mL). The organic layer was dried over anhydrous $MgSO_4$, filtered, and concentrated to dryness to afford 1.20 g of 12-cyclopropyldodecylmethanesulfonate (89%). The crude mesylate was used in the next step without further purification. ^{1}H NMR (300 MHz, $CDCl_3$): δ 4.22 (t, J = 6.0 Hz, 2 H), 3.01 (s, 3 H), 1.74 (m, 2 H), 1.27 (bm, 20 H), 0.64 (m, 1 H), 0.38 (m, 2 H), −0.01 (m, 2 H).

12-Bromododecylcyclopropane. The crude mesylate (1.20 g, 3.94 mmol) and lithium bromide (1.02 mg, 11.8 mmol) were dissolved in reagent grade acetone (50 mL) and refluxed overnight. The solvent was removed by rotary evaporation. Water (100 mL) and diethyl ether (50 mL) were added to dissolve the salt and the product, respectively. The aqueous layer was extracted with diethyl ether (3 × 50 mL). The combined organic layers were washed with brine (200 mL), dried over anhydrous $MgSO_4$, filtered, and concentrated to dryness. The crude product was purified by column chromatography on silica gel (hexanes, R_f = 0.72) to afford 1.10 g of 12-bromododecylcyclopropane (97%). ^{1}H NMR (300 MHz, $CDCl_3$): δ 3.41 (t, J = 7.2 Hz, 2 H), 1.85 (m, 2 H), 1.26 (bm, 20 H), 0.65 (m, 1 H), 0.38 (m, 2 H), −0.02 (m, 2 H).

12-Cyclopropyldodecylthioacetate. Potassium thioacetate (0.87 g, 7.6 mmol) was dissolved in 50 mL of absolute ethanol (previously degassed) under argon. The crude bromide (1.10 g, 3.82 mmol) diluted with degassed absolute ethanol was added dropwise to potassium thioacetate solution over 5 min. The reaction mixture was stirred under reflux for 4 h. After cooling, the precipitate was filtered off and rinsed with ethanol, and the resulting organic phase was evaporated to dryness. The residue was taken up with a mixture of hexanes (100 mL) and water (100 mL). The aqueous layer was extracted with hexanes (3 × 50 mL), and the combined organic layers were washed with brine (100 mL), dried over anhydrous $MgSO_4$, filtered, and evaporated to dryness. The crude product was purified using column chromatography on silica gel (hexanes, R_f = 0.2) to afford 0.50 g of 12-cyclopropyldodecylthioacetate (46%) as a white solid. ^{1}H NMR (300 MHz, $CDCl_3$): δ 2.86 (t, J = 6.9 Hz, 2 H), 2.32 (s, 3 H), 1.55 (m, 2 H), 1.25 (bm, 20 H), 0.64 (m, 1 H), 0.37 (m, 2 H), −0.03 (m, 2 H).

12-Cyclopropyldodecanethiol. An aliquot of 12-cyclopropyldodecylthioacetate (0.50 g, 1.8 mmol) diluted in dry THF (10 mL) was carefully added to a suspension of lithium aluminum hydride (100 mg, 2.64 mmol) in dry THF (10 mL) at 0 °C. The reaction mixture was stirred for 4 h at room temperature under argon. After completion, the reaction mixture was cooled to 0 °C, quenched with water (20 mL), and acidified to pH ~1 using dilute HCl (50 mL) under an argon atmosphere. The mixture was left stirring until the precipitate was completely dissolved. The aqueous layer was extracted with hexanes (3 × 50 mL) and the combined organic layers were washed with brine (100 mL), dried over anhydrous $MgSO_4$, filtered, and concentrated to dryness. The residue was purified by column chromatography on silica gel (hexanes, R_f = 0.54) to afford 0.40 g of 12-cyclopropyldodecanethiol (94%). ^{1}H NMR (300 MHz, $CDCl_3$): δ 2.52 (q, J = 7.5 Hz, 2 H), 1.60 (quintet, J = 7.5 Hz, 2 H), 1.33 (t, J = 7.5 Hz, 1 H), 1.26 (bs, 18 H), 1.17 (q, J = 6.9 Hz, 2 H), 0.64 (m, 1 H), 0.38 (m, 2 H), −0.02 (m, 2 H). ^{13}C NMR (75 MHz, $CDCl_3$): δ 34.8, 34.1, 29.7, 29.65, 29.57, 29.55, 29.5, 29.1, 28.4, 24.7, 10.4, 4.3.

9-Cyclopropylnonanethiol. ^{1}H NMR (300 MHz, $CDCl_3$): δ 2.52 (q, J = 7.5 Hz, 2 H), 1.60 (quintet, J = 7.5 Hz, 2 H), 1.33 (t, J = 7.5 Hz, 1 H), 1.26 (bs, 12 H), 1.17 (q, J = 7.0 Hz, 2 H), 0.64 (m, 1 H), 0.37 (m, 2 H), −0.02 (m, 2 H). ^{13}C NMR (75 MHz, $CDCl_3$): δ 34.8, 34.0, 29.63, 29.61, 29.5, 29.1, 28.4, 24.7, 10.9, 4.3.

10-Cyclopropyldecanethiol. ^{1}H NMR (300 MHz, $CDCl_3$): δ 2.52 (q, J = 7.5 Hz, 2 H), 1.61 (quintet, J = 7.5 Hz, 2 H), 1.33 (t, J = 7.5 Hz, 1 H), 1.27 (bs, 14 H), 1.17 (q, J = 6.9 Hz, 2 H), 0.64 (m, 1 H), 0.38 (m, 2 H), −0.02 (m, 2 H). ^{13}C NMR (75 MHz, $CDCl_3$): δ 34.8, 34.1, 29.7, 29.64, 29.58, 29.5, 29.1, 28.4, 24.7, 10.9, 4.4.

11-Cyclopropylundecanethiol. ^{1}H NMR (300 MHz, $CDCl_3$): δ 2.52 (q, J = 7.5 Hz, 2 H), 1.60 (quintet, J = 7.5 Hz, 2 H), 1.33 (t, J = 7.5 Hz, 1 H), 1.26 (bs, 16 H), 1.17 (q, J = 7.0 Hz, 2 H), 0.64 (m, 1 H), 0.38 (m, 2 H), −0.02 (m, 2 H). ^{13}C NMR (75 MHz, $CDCl_3$): δ 34.8, 34.1, 29.69, 29.66, 29.64, 29.59, 29.53, 29.51, 29.1, 28.4, 24.7, 10.9, 4.4.

13-Cyclopropyltridecanethiol. ^{1}H NMR (300 MHz, $CDCl_3$): δ 2.52 (q, J = 7.5 Hz, 2 H), 1.61 (quintet, J = 7.5 Hz, 2 H), 1.33 (t, J = 7.5 Hz, 1 H), 1.26 (bs, 20 H), 1.17 (q, J = 6.9 Hz, 2 H), 0.64 (m, 1 H), 0.38 (m, 2 H), −0.02 (m, 2 H). ^{13}C NMR (75 MHz, $CDCl_3$): δ 34.8, 34.1, 29.7, 29.65, 29.57, 29.55, 29.5, 29.1, 28.4, 24.7, 10.9, 4.3.

Synthesis of 13-Tetradecenyl Disulfide. As illustrated in Scheme 2, the preparation of 13-tetradecenyl disulfide (n = 12) begins with the synthesis of (11-bromoundecyloxy)tert-butyldimethylsilane. A mixture of 11-bromo-1-undecanol (3.0 g, 12 mmol), *tert*-butyldimethylsilyl chloride (TBDMSCl; 1.99 g, 13.2 mmol), triethylamine (1.92 mL, 13.8 mmol), and 4-dimethylaminopyridine (0.059 g, 0.48 mmol) in dichloromethane was stirred overnight at room temperature under argon. After evaporation of solvent, the residue was taken up using a mixture of diethyl ether (100 mL) and 10% aqueous HCl (100 mL). The organic layer was washed with 10% aqueous HCl (3 × 100 mL), dried over anhydrous $MgSO_4$, and concentrated to dryness. The crude product was purified by column chromatography on silica gel (2% diethyl ether/hexanes, R_f = 0.3) to afford 4.1 g of (11-bromoundecyloxy)-*tert*-butyldimethylsilane (98%) as a viscous oil. ^{1}H NMR (300 MHz, $CDCl_3$): δ 3.59 (t, J = 6.6 Hz, 2 H), 3.41 (t, J = 6.9 Hz, 2 H), 1.85 (m, 2 H), 1.46 (m, 2 H), 1.27 (bm, 14 H), 0.89 (s, 9 H), 0.05 (s, 6 H).

Tert-butyldimethyl(13-tetradecenyloxy)silane. An aliquot of (11-bromoundecyloxy)*tert*-butyldimethylsilane (1.20 g, 3.30 mmol) was dissolved in dry THF (10 mL), and the catalyst Li_2CuCl_4 (0.1 M in THF, 1.32 mL, 0.132 mmol) was added to the solution under argon. The mixture was left stirring at room temperature for 20 min, and allyl magnesium chloride (2.0 M solution in THF, 3.30 mL, 6.60 mmol) was then added dropwise over 15 min. The reaction mixture turned from bright orange to colorless at the beginning, and then to brown as an excess of Grignard reagent was added. The reaction was left stirring overnight at room temperature under argon to ensure completion. The flask was cooled in an ice bath, and the reaction was quenched with saturated aqueous NH_4Cl (100 mL). The aqueous layer was extracted with hexanes (3 × 50 mL), and the combined organic layers were washed with brine (200 mL), dried over anhydrous $MgSO_4$, and concentrated to dryness. The crude *tert*-butyldimethyl(13-tetradecenyloxy)silane (1.0 g, 86%) was used in the next step without further purification. ^{1}H NMR (300 MHz, $CDCl_3$): δ 5.78−5.83 (m, 1 H), 4.90−5.02 (m, 2 H), 3.59 (t, J = 6.6 Hz, 2 H), 2.03 (m, 2 H), 1.50 (m, 2 H), 1.25 (bm, 18 H), 0.89 (s, 9 H), 0.04 (s, 6 H).

13-Tetradecenol. *Tert*-butylammonium fluoride (TBAF; 1.0 M solution in THF, 5.77 mL, 5.77 mmol) was added to a stirred solution of *tert*-butyldimethyl(13-tetradecenyloxy)silane (1.0 g, 2.2 mmol) in dry THF (15 mL). The stirring was continued for 2 h at room temperature under argon. The solution was then poured into water (100 mL) and extracted with ethyl acetate (3 × 50 mL). The combined organic phase was washed with brine (100 mL), dried over anhydrous $MgSO_4$, and concentrated to dryness. The crude 13-tetradecenol (0.38 g, 86%) was used in the next step without further purification. ^{1}H NMR (300 MHz, $CDCl_3$): δ 5.78−5.83 (m, 1 H), 4.90−5.02 (m, 2 H), 3.64 (t, J = 6.6 Hz, 2 H), 2.02 (m, 2 H), 1.55 (m, 2 H), 1.26 (bm, 18 H).

13-Tetradecenylmethanesulfonate. To an aliquot of 13-tetradecenol (0.38 g, 1.8 mmol) diluted in 50 mL of hexanes was slowly added an aliquot (1.25 mL, 8.95 mmol) of triethylamine. The reaction mixture was left stirring at room temperature for 30 min. The solution was cooled in an ice bath, and then an aliquot (0.42 mL, 5.4 mmol) of methanesulfonyl chloride was added dropwise. The reaction mixture was stirred for 4 h at room temperature to ensure completion. Excess methanesulfonyl chloride was destroyed by adding a small aliquot of water, and the precipitate was dissolved by adding 100 mL of water. The organic layer was separated, and the aqueous layer was extracted with diethyl ether (3 × 50 mL). The combined organic layers were washed with dilute HCl (100 mL), saturated aqueous $NaHCO_3$ (50 mL), and brine (100 mL). The organic layer was dried over anhydrous $MgSO_4$, filtered, and concentrated to dryness to afford 0.55 g of crude 13-tetradecenylmethanesulfonate (106%), which was used in the next step without further purification. ^{1}H NMR (300 MHz, $CDCl_3$): δ 5.79−5.85 (m, 1 H), 4.93−5.05 (m, 2 H), 4.25 (t, J = 6.6 Hz, 2 H), 3.03 (s, 3 H), 2.05 (m, 2 H), 1.77 (m, 2 H), 1.29 (bm, 18 H).

13-Tetradecenylthioacetate. Potassium thioacetate (0.432 g, 3.80 mmol) was dissolved in 20 mL of absolute ethanol (previously degassed) under argon. The crude mesylate (0.55 g, 1.9 mmol) diluted with degassed absolute ethanol was added dropwise to the stirred solution over 5 min. The reaction mixture was stirred under reflux for 4 h. After cooling, the precipitate was filtered off and rinsed with ethanol. The resulting organic phase was evaporated to dryness. The residue was taken up with a mixture of hexanes (100 mL) and water (100 mL). The aqueous layer was extracted with hexanes (3 × 30 mL), and the combined organic layers were washed with brine (100 mL), dried over anhydrous $MgSO_4$, filtered, and evaporated to dryness. The crude product was purified using column chromatography on silica gel (hexanes, R_f = 0.18) to afford 0.40 g of 13-tetradecenylthioacetate (78%) as a white solid. ^{1}H NMR (300 MHz, $CDCl_3$): δ 5.79−5.85 (m, 1 H), 4.92−5.03 (m, 2 H), 2.87 (t, J = 7.2 Hz, 2 H), 2.33 (s, 3 H), 2.03 (m, 2 H), 1.52 (m, 2 H), 1.26 (bm, 18 H).

13-Tetradecenyl Disulfide. An aliquot of 13-tetradecenylthioacetate (0.40 g, 1.5 mmol) diluted in dry THF (10 mL) was carefully added to a suspension of lithium aluminum hydride (84 mg, 2.2 mmol) in dry THF (10 mL) at 0 °C. The reaction mixture was stirred for 4 h under argon at room temperature. The reaction mixture was quenched with water (20 mL) at 0 °C, and then acidified to pH ∼1 using dilute HCl (50 mL) in air. The mixture was left stirring until the precipitate was completely dissolved at 0 °C. The aqueous layer was extracted with hexanes (3 × 50 mL) and the combined organic layers were washed with brine (100 mL), dried over anhydrous $MgSO_4$, filtered, and concentrated to dryness. The residue was purified by column chromatography on silica gel (hexanes, R_f = 0.67) to afford 108 mg of 13-tetradecenyl disulfide (32%). ^{1}H NMR (300 MHz, $CDCl_3$): δ 5.77−5.86 (m, 2 H), 4.90−5.02 (m, 4 H), 2.51 (t, J = 6.9 Hz, 4 H), 2.04 (m, 4 H), 1.67 (m, 4 H), 1.26 (bs, 36 H).

14-Pentadecenyl Disulfide. ^{1}H NMR (300 MHz, $CDCl_3$): δ 5.79−5.83 (m, 2 H), 4.90−5.02 (m, 4 H), 2.51 (t, J = 7.2 Hz, 4 H), 2.03 (m, 4 H), 1.58 (m, 4 H), 1.26 (bs, 40 H).

Synthesis of 12-Isopropyldodecanethiol. As illustrated in Scheme 3, the synthesis of 12-isopropyldodecanethiol (n = 12) begins with the preparation of 11-(tert-butyldimethylsilyloxy)undecylphosphonium bromide. A mixture of (11-bromoundecyloxy)*tert*-butyldimethylsilane (1.50 g, 4.12 mmol) and triphenylphosphine (1.62 g, 6.18 mmol) was stirred neat at 95 °C overnight under argon. After cooling, excess triphenylphosphine and unreacted materials were removed through trituration with dry diethyl ether. Any residual water was removed by azeotropic distillation with benzene. The phosphonium bromide (2.17 g, 84%) was used in the next step without further purification.

Tert-butyldimethyl(12-isopropyl-11-dodecenyloxy)silane. The crude phosphonium bromide (2.17 g, 3.46 mmol) was dissolved in dry THF (25 mL) and cooled to −78 °C under argon. An aliquot of *n*-BuLi (1.60 M in hexanes, 2.80 mL, 4.50 mmol) was added dropwise and stirring was continued for an additional 30 min at −40 °C. The resulting bright orange ylide solution was cooled to −78 °C and treated with isobutyraldehyde (0.628 mL, 6.92 mmol). The reaction mixture was stirred at room temperature overnight. The resulting slurry was filtered, and the precipitate was washed with THF. The filtrate was concentrated to dryness, and the residue was triturated with hexanes to remove triphenylphosphine oxide. The organic phase was evaporated to dryness, and the residue was purified using column chromatography on silica gel (hexanes, R_f = 0.24) to afford *tert*-butyldimethyl(12-isopropyl-11-dodecenyloxy)silane (0.50 g, 42%) as a colorless oil. ^{1}H NMR (300 MHz, $CDCl_3$): δ 3.60 (t, J = 6.6 Hz, 2 H), 3.19 (t, J = 6.9 Hz, 2 H), 1.82 (m, 2 H), 1.50 (m, 2 H), 1.26 (bs, 14 H), 0.90 (s, 9 H), 0.05 (s, 6 H).

12-Isopropyl-11-dodecenol. TBAF (1.0 M solution in THF, 2.90 mL, 2.90 mmol) was added to a stirred solution of *tert*-butyldimethyl(12-isopropyl-11-dodecenyloxy)silane (0.50 g, 1.5 mmol) in dry THF (10 mL) at room temperature and the stirring was continued for 2 h under argon. The mixture was then poured into water (100 mL) and extracted with ethyl acetate (3 × 50 mL). The combined organic phase was washed with brine (100 mL), dried over anhydrous $MgSO_4$, and concentrated to dryness. The crude 12-isopropyl-11-dodecenol (0.33 g, 100%) was used in the next step without further purification. ^{1}H NMR (300 MHz, $CDCl_3$): δ 5.2 (m, 2 H), 3.62 (t, J = 6.3 Hz, 2 H), 2.58 (m, 1 H), 2.03 (m, 2 H), 1.54 (m, 2 H), 1.38−1.22 (m, 14 H), 0.88 (d, J = 6.6 Hz, 6 H).

12-Isopropyldodecanol. To a stirred suspension of Pd/C (100 mg) in dichloromethane (20 mL) activated with hydrogen was added an aliquot of 12-isopropyl-11-dodecenol (0.33 g, 1.5 mmol). The mixture was stirred under a small overpressure of hydrogen for 1 h at room temperature. The solid was filtered through a plug of silica gel, and the residue was diluted with 50 mL of dichloromethane and cooled to 0 °C in an ice bath. Ozone was bubbled through the solution for 10 min. The disappearance of olefinic moiety was monitored by ^{1}H NMR spectroscopy by taking an aliquot of the reaction mixture. After bubbling argon through the solution for 10 min, the solvent was evaporated at room temperature under vacuum. Methanol (20 mL) was added to dissolve the residue and an aliquot of sodium borohydride (100 mg) was added to the cooled solution. The mixture was stirred overnight at room temperature under argon then ice−water (200 mL) was added to quench the reaction. The mixture was neutralized with concentrated HCl and extracted with hexanes (3 × 100 mL). The combined organic layers were washed with brine (200 mL), dried over anhydrous $MgSO_4$, and concentrated to dryness. The crude product was purified using column chromatography on silica gel (diethyl ether/hexanes = 1/2, R_f = 0.33) to afford 12-isopropyldodecanol (0.31 g, 92%). ^{1}H NMR (300 MHz, $CDCl_3$): δ 3.62 (t, J = 6.3 Hz, 2 H), 1.59−1.43 (m, 4 H), 1.37−1.10 (m, 20 H), 0.88 (d, J = 6.6 Hz, 6 H).

12-Isopropyldodecylmethanesulfonate. To an aliquot of 12-isopropyldodecanol (0.31 g, 1.3 mmol) diluted in 50 mL of hexanes was slowly added an aliquot (0.93 mL, 6.7 mmol) of triethylamine. The reaction mixture was left stirring at room temperature for 30 min. The solution was cooled in an ice bath, and then an aliquot (0.31 mL, 4.0 mmol) of methanesulfonyl chloride was added dropwise. The reaction was stirred for 4 h at room temperature to ensure completion. Excess methanesulfonyl chloride was destroyed using small aliquot of water, and the precipitate was dissolved using 200 mL of water. The

organic layer was separated, and the aqueous layer was extracted with diethyl ether (3 × 50 mL). The combined organic layers were washed with dilute HCl (300 mL), saturated aqueous $NaHCO_3$ (200 mL), and brine (300 mL). The organic layer was dried over $MgSO_4$, filtered, and concentrated to dryness to afford 0.36 g of crude mesylate (88%), which was used in the next step without further purification. ^{1}H NMR (300 MHz, $CDCl_3$): δ 4.20 (t, J = 6.9 Hz, 2 H), 2.98 (s, 3 H), 1.73 (m, 2 H), 1.50 (m, 1 H), 1.40−1.10 (m, 20 H), 0.88 (d, J = 6.6 Hz, 6 H).

12-Isopropyldodecylthioacetate. Potassium thioacetate (0.40 g, 3.5 mmol) was dissolved in 50 mL of absolute ethanol (previously degassed) under argon. The crude mesylate (0.36 g, 1.2 mmol) was added dropwise to the stirred solution over 5 min. The reaction mixture was stirred under reflux for 4 h. After cooling, the precipitate was filtered off and rinsed with ethanol. The resulting organic phase was evaporated to dryness. The residue was taken up with a mixture of hexanes (100 mL) and water (100 mL). The aqueous layer was extracted with hexanes (3 × 50 mL). The combined organic layers were washed with brine (100 mL), dried over anhydrous $MgSO_4$, filtered, and evaporated to dryness. The crude product was purified using column chromatography on silica gel (hexanes, R_f = 0.26) to afford 12-isopropyldodecylthioacetate (0.301 g, 90%) as a white solid. ^{1}H NMR (300 MHz, $CDCl_3$): δ 2.87 (t, J = 7.2 Hz, 2 H), 2.33 (s, 3 H), 2.03 (m, 2 H), 1.50 (m, 1 H), 1.39−1.10 (m, 20 H), 0.88 (d, J = 6.6 Hz, 6 H).

12-Isopropyldodecanethiol. An aliquot of 12-isopropyldodecylthioacetate (0.301 g, 1.05 mmol) diluted in dry THF (10 mL) was carefully added to a suspension of lithium aluminum hydride (59 mg, 1.6 mmol) in dry THF (10 mL) cooled in an ice bath. The reaction mixture was stirred for 4 h under argon. The reaction mixture was cooled to 0 °C, quenched with a few milliliters of water, and acidified to pH ~1 using dilute HCl. The mixture was left stirring under argon until the precipitate was completely dissolved. The aqueous layer was extracted with hexanes (3 × 50 mL), and the combined organic layers were washed with brine (2 × 200 mL), dried over anhydrous $MgSO_4$, filtered, and concentrated to dryness to afford 220 mg of 12-isopropyldodecanethiol (87%). ^{1}H NMR (300 MHz, $CDCl_3$): δ 2.50 (q, J = 7.5 Hz, 2 H), 1.64−1.43 (m, 3 H), 1.38−1.10 (m, 21 H), 0.85 (d, J = 6.6 Hz, 6 H). ^{13}C NMR (75 MHz, $CDCl_3$): δ 39.0, 34.0, 29.9, 29.7, 29.63, 29.57, 29.5, 29.1, 28.4, 28.0, 27.4, 24.6, 22.6.

13-Isopropyltridecanethiol. ^{1}H NMR (300 MHz, $CDCl_3$): δ 2.50 (q, J = 7.4 Hz, 2 H), 1.65−1.44 (m, 3 H), 1.36−1.05 (m, 23 H), 0.86 (d, J = 6.6 Hz, 6 H). ^{13}C NMR (75 MHz, $CDCl_3$): δ 39.1, 34.1, 29.9, 29.8, 29.7, 29.6, 29.4, 29.1, 28.4, 28.0, 27.5, 24.7, 22.7.

Substrate Preparation. Gold substrates were prepared by thermal evaporation of 1000 Å of gold onto silicon wafers Si(111), precoated with an adhesion layer of chromium (100 Å). The deposition was carried out at a rate of 1 Å/s under ultrahigh vacuum conditions. The resulting gold-coated wafers were rinsed with absolute ethanol and blown dry with ultrahigh purity nitrogen gas prior to adsorption of the thiols.

Sample Preparation. Ethanolic solutions of each thiol at 1 mM concentration were prepared in glass vial, which were previously cleaned with piranha solution (H_2SO_4:H_2O_2 = 3:1). **Caution:** *Piranha solution can react violently with organic compounds and should be handled with care.* The clean gold-coated wafers were immersed in the thiol solutions for 24 h, after which they were rinsed with absolute ethanol and blown dry with ultrahigh purity nitrogen gas before characterization.

Ellipsometric Thickness Measurements. A Rudolph Research Auto EL III ellipsometer operating with a 632.8 nm He−Ne laser at an incident angle of 70° from the surface normal was employed to measure the thickness of the SAMs. A refractive index of 1.45 was assumed for all films. The reported values represent the average of at least 12 measurements and were reproducible within ±2 Å.

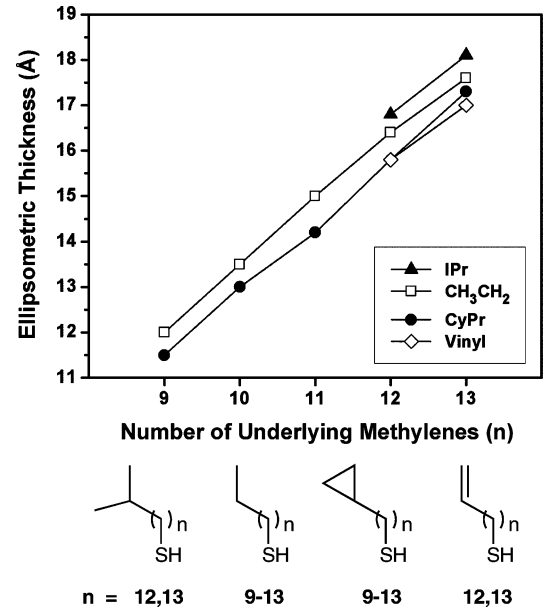

FIGURE 1. Ellipsometric thicknesses for analogous isopropyl-, methyl-, cyclopropyl-, and vinyl-terminated SAMs.

Contact Angle Measurements. Contacting liquids were dispensed onto the surface of the SAMs using a Matrix Technologies micro-Electrapette 25. Advancing and receding contact angles were measured with a ramé-hart model 100 goniometer with the pipet tip in contact with the drop of liquid. The reported are the average of at least 12 measurements and were reproducible within ±1°.

Polarization Modulation Infrared Reflection Absorption Spectroscopy (PM-IRRAS). A Nicolet MAGNA-IR 860 Fourier-transform spectrometer equipped with a liquid nitrogen-cooled mercury−cadmium−telluride (MCT) detector and a Hinds Instruments PEM-90 photoelastic modulator (37 Hz) was employed to acquire the PM-IRRAS spectra. The data were collected at a spectral resolution of 4 cm^{-1} for 256 scans using p-polarized light reflected from the sample at an angle of incidence of 80° from the surface normal.

Preparation of Polyethylene (PE) Films. Polyethylene (PE - linear, MW ~52 000) in pellet form was purchased from Polysciences, Inc. The pellets were flattened by pressing with a mechanical press at a pressure of 10 000 psi to produce thin sheets of PE. The sheets were further processed by mounting the material in a mechanical vice sandwiched between two polished metal surfaces for one hour at a temperature of 150 °C. This procedure created flat PE surfaces that maintained their profile throughout the ensuing experimental analysis.

RESULTS AND DISCUSSION

Ellipsometric Thicknesses. Figure 1 summarizes the ellipsometric thicknesses of SAMs on gold derived from the series of newly prepared ω-cyclopropylalkanethiols as well as the thicknesses of SAMs derived from normal alkanethiols of similar chain length. For comparison, we also included thickness data for two representative vinyl-terminated SAMs and two representative isopropyl-terminated SAMs. As the number of CH_2 groups increases from 9 to 13, the thickness increases in a systematic fashion. For the cyclopropyl-terminated SAMs, the plot gives a slope of 1.5 Å per CH_2 unit. Both the calculated slope and the absolute thicknesses are

in good agreement with those previously observed in the widely investigated normal alkanethiol SAMs on gold (37, 38). Comparison of the cyclopropyl-terminated SAMs to the methyl-terminated SAMs reveals that the thicknesses of the former are slightly lower by ~0.5 Å for all chain lengths examined.

To rationalize this small but reproducible difference, we first assume that the chain tilt (~30°) (18) and the conformational order of all of the films are similar (both assumptions are consistent with our analysis by PM-IRRAS; vide infra). We also know that the terminal C−C bond length is unusually short for the cyclopropyl ring (i.e., 1.515 Å for cyclopropyl vs 1.545 Å for CH_3CH_2) (35), and the HCH bond angle is expanded to 114.5° (35). Simple modeling as an equilateral triangle reveals that the shortest diagonal between the ring carbons and the opposite edge of a cyclopropyl ring is ~1.31 Å. Correspondingly, projection in the plane normal to the surface predicts that a cyclopropyl terminal group in a SAM on gold should be shorter by ~0.2 Å than an analogous terminal CH_3CH_2 group (i.e., 1.13 Å for cyclopropyl vs 1.34 Å for ethyl) (39). This difference alone, however, is insufficient to account for the reproducibly observed difference in thickness of ~0.5 Å.

Although it is plausible that the steric bulk of the cyclopropyl groups might disrupt the interchain packing and give rise to an anomalously low ellipsometric thickness, we note that the SAMs terminated with even bulkier isopropyl groups (40) show the opposite trend (see Figure 1). Furthermore, SAMs terminated with sterically smaller vinyl groups (40, 41) exhibit thicknesses similar to those of the cyclopropyl-terminated SAMs (and thus diminished thicknesses compared to the corresponding CH_3CH_2-terminated SAMs). Like the cyclopropyl-terminated SAMs, this latter phenomenon can be attributed in part to the vinyl group's diminished terminal bond length (i.e., the length of the terminal C═C bond is 1.34 Å rather than 1.54 Å) (35) and its expanded HCH bond angle (120°) (35). Notably, vinyl and cyclopropyl groups are more conformationally restricted (i.e., rigid) when compared to ethyl and isopropyl groups, respectively. Nevertheless, the steric bulk of a vinyl group is less than that of an ethyl group (41), and the steric bulk of each of these groups is less than that of a cyclopropyl group (40, 41).

Polarization Modulation Infrared Reflection Absorption Spectroscopy (PM-IRRAS). Infrared reflectance spectra in the C−H stretching region of SAMs derived from the series of ω-cyclopropylalkanethiols are shown in Figure 2. The first striking observation is that the vibrations corresponding to the stretching of the methylene groups in the ring are blue-shifted (i.e., 3000−3100 cm^{-1}) relative to the methylene groups along the chain backbone (i.e., 2850−2920 cm^{-1}), as detailed in Table 1. This shift was also observed in the transmission IR spectra of the corresponding thiols as illustrated in Figure 3.

Generally, for cyclopropane, to relieve the strain associated with the sharp angle between carbons in the ring (60°), the four sp^3 hybrid orbitals of carbon are nonequivalent. There is a greater degree of p character for the internal

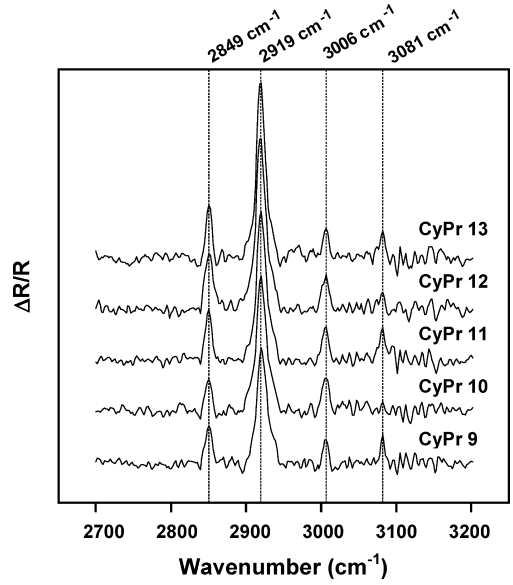

FIGURE 2. PM-IRRAS spectra of cyclopropyl-terminated SAMs of increasing chain length.

Table 1. Peak Assignments (cm^{-1}) for the PM-IRRAS Spectra of the Cyclopropyl-Terminated SAMs

assignment	CyPr 9	CyPr 10	CyPr 11	CyPr 12	CyPr 13
CH_2 sym stretch	2850	2850	2850	2850	2850
CH_2 antisym stretch	2919	2919	2918.5	2918	2918
CH_2 cycle sym stretch	3004.5	3006.5	3006.5	3006.5	3006.5
CH_2 cycle antisym stretch	3081.5		3081.5	3081.5 (w)	3081.5

orbitals involved in the formation of C−C bonds to relieve the small-angle strain; these orbitals are referred to as ~sp^5 orbitals (35). Correspondingly, the p character decreases in the external hybrid orbitals involved in C−H bond formation, rendering them similar to ~sp^2 orbitals (35, 42). These characteristics are supported by the PM-IRRAS spectra of the cyclopropyl- and vinyl-terminated SAMs (see Figure 4). In particular, the positions of the cyclic CH_2 stretching bands (3000−3100 cm^{-1}) of the cyclopropyl-terminated films and those of the terminal and internal olefinic C−H stretching

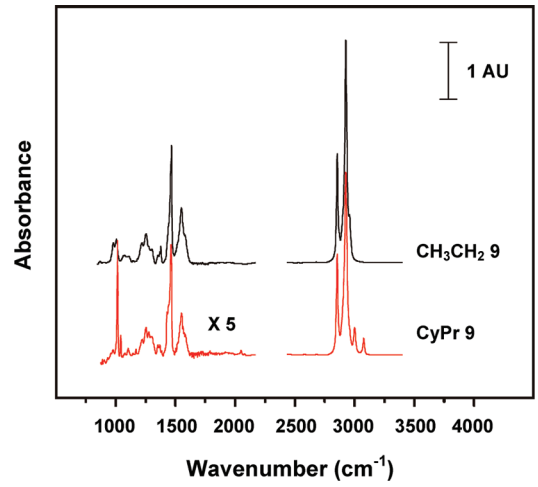

FIGURE 3. Transmission IR of cyclopropyl- and methyl-terminated SAMs: $CyPr(CH_2)_9SH$ and $CH_3CH_2(CH_2)_9SH$.

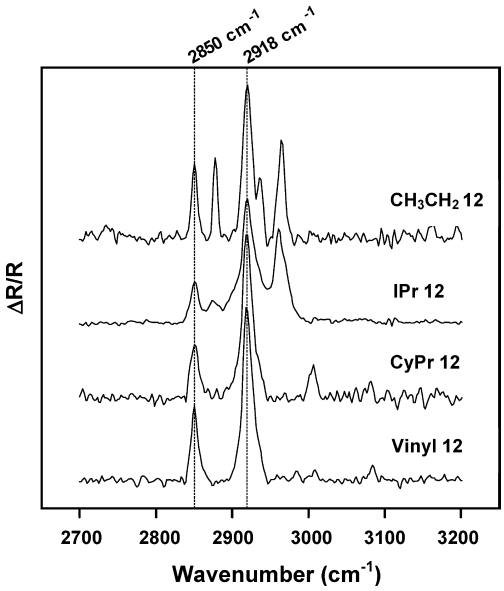

FIGURE 4. Comparison of the PM-IRRAS spectra for methyl-, isopropyl-, cyclopropyl-, and vinyl-terminated SAMs of identical chain length ($n = 12$).

Table 2. Peak Assignments (cm^{-1}) for the PM-IRRAS Spectra of Methyl-, Vinyl-, and Isopropyl-terminated SAMs, When $n = 12$

assignment	$CH_3CH_2$12	Vinyl 12	IPr 12
$CH_{2\ sym\ stretch}$	2850	2850	2850
$CH_{3\ sym\ stretch}$	2877.5		2873.5 (w)
$CH_{2\ antisym\ stretch}$	2918	2919	2919
$CH_{3\ antisym\ stretch}$	2964		2960 (s,br)
$C{=}CH_{2\ sym\ stretch}$		2983 (w)	
$H{-}C{=}C_{stretch}$		3008 (w)	
$C{=}CH_{2\ antisym\ stretch}$		3083	

bands (2980−3100 cm^{-1}) of the vinyl-terminated films are nearly identical (see also Table 2). Interestingly, although vinyl-terminated SAMs are known (43, 44), information regarding the orientation of the terminal group with respect to the surface has yet to be reported.

For long aliphatic chains and polymers, Snyder and coworkers demonstrated that the position of the antisymmetric CH_2 stretch varies systematically with the number of gauche defects along the methylene chain (45). More precisely, a crystalline sample of stretched polymer chains shows a sharp band at 2918 cm^{-1}; in contrast, a liquidlike environment for the chains shows a broad peak that is blue-shifted to 2926 cm^{-1} (45). Similarly, for SAMs derived from normal alkanethiols on gold, the conformational order of the films can be evaluated from the position of the antisymmetric stretching band as well as its width at half height (fwhm) (46). For our cyclopropyl-terminated SAMs, the antisymmetric CH_2 stretching band undergoes a red shift from 2919 to 2918 cm^{-1} as the number of methylene groups increases from 9 to 13 (see Figure 2 and Table 1). This trend can be rationalized by the increase in interchain van der Waals interactions that accompanies the increase in chain length, giving rise to an increase in the conformational order or "crystallinity" of the films. Notably, the increase in intensity

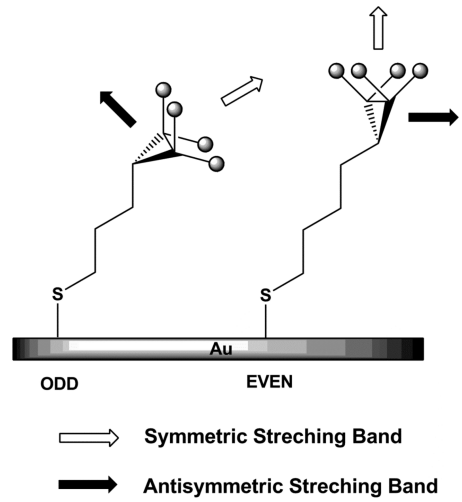

FIGURE 5. Proposed orientation of the cyclopropyl terminal group on the surfaces with odd- and even-numbered chains and the corresponding transition dipoles of the methylene vibrations.

of this band (Figure 2) directly reflects the increase in the number of methylene units in the chains.

In the PM-IRRAS spectra of the cyclopropyl-terminated SAMs (Figure 2), there is a small but reproducible "odd−even" effect in the cyclic CH_2 stretching region (3000−3100 cm^{-1}) (47, 48). In particular, the films with even-numbered chain lengths show a greater intensity ratio for the symmetric cyclic CH_2 stretch (3006 cm^{-1}) vs the antisymmetric cyclic CH_2 stretch (3081 cm^{-1}). This phenomenon can be rationalized by considering the orientation of the cyclic methylene groups relative to the surface normal. When a molecule is adsorbed on a substrate, the molecule induces opposite image charges in the substrate (49). The dipole moment of the molecule and the image charges perpendicular to the surface reinforce each other. In contrast, the dipole moments of the molecule and the image charges parallel to the surface cancel out. Therefore, the surface selection rule states that only vibrations that involve changes in dipole moment perpendicular to the surface can be detected and observed in the vibrational spectrum (50, 51). Examination of the transmission IR for all cyclopropyl-terminated thiols (data not shown) revealed no significant difference in the intensity of the peaks associated with the symmetric and antisymmetric stretches of the cyclic methylenes. Therefore, the observed "odd−even" effect appears to arise exclusively from the differences in the orientation of the ring with respect to the surface normal.

Further, when considering the relative orientation of the ring with respect to the surface normal, we can predict that the ring will tilt more for adsorbates containing an odd number of carbon atoms in the backbone (i.e., counting only the CH_2 groups between the sulfur headgroup and the terminal cyclopropyl ring), while the even-numbered chains produce surfaces with the rings oriented largely perpendicular to the surface (see Figure 5). Because of the symmetry of cyclopropyl group, the cyclic CH_2 symmetric stretch is oriented directly along the bisector of the ring and within the plane defined by the main axis of the molecule, whereas the cyclic CH_2 antisymmetric stretch is perpendicular to the

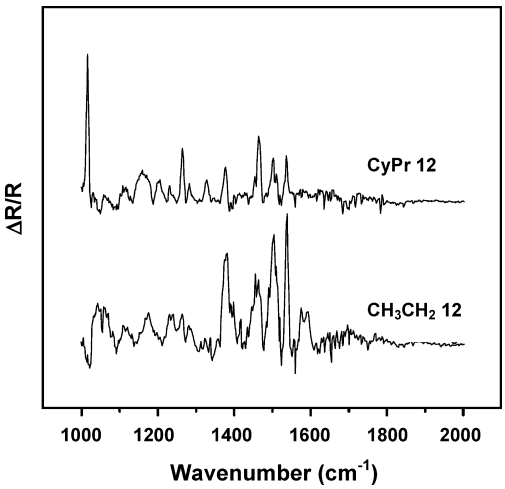

FIGURE 6. Comparison of the PM-IRRAS spectra in the C−C stretching region for methyl- and cyclopropyl-terminated SAMs, where $n = 12$.

ring as illustrated in Figure 5. Thus, for SAMs generated from the even-numbered chains, the orientation of the ring is such that the intensity of the symmetric stretching band is maximized compared to the antisymmetric band, whereas the opposite is true for SAMs generated from the odd-numbered backbones.

Figure 4 highlights the fact that the backbone CH_2 antisymmetric (2918 cm^{-1}) and symmetric (2850 cm^{-1}) stretches for all of the films appear at roughly the same band position, and the magnitude of the fwhm is also similar. In case of the isopropyl-terminated SAMs, this observation agrees with the conclusion by Kim et al. that large isopropyl terminal groups fail to perturb the packing structure of SAMs on gold (52). Our spectral data suggest that this conclusion is also valid for cyclopropyl- and vinyl-terminated SAMs on gold. Even though we are unable to determine the precise orientation of the terminal vinyl and isopropyl groups from the PM-IRRAS spectra, we can conclude with confidence that the conformational order of the methylene backbones is similar for all of the films generated in this investigation.

Spectra of representative methyl- and cyclopropyl-terminated SAMs in the C−C stretching region (1000−2000 cm^{-1}) are shown in Figure 6. The most obvious difference between the two spectra is the presence of a strong band at 1016 cm^{-1} in the latter SAM, which can be assigned to a cyclopropyl ring vibration (47). Because the intensity of this band is roughly the same for all of the cyclopropyl-terminated SAMs examined (data not shown) and in the transmission IR spectra of the cyclopropyl-terminated thiols (e.g., Figure 3), the change in the dipole moment associated with this ring vibration must be unaffected by the orientation of the ring with respect to the surface. A second difference between the two spectra in Figure 6 is the weak band at 1274 cm^{-1} in the cyclopropyl-terminated SAM, which is associated with a CH_2 deformation mode for the cyclic CH_2 groups (48). Other bands are either weak or are associated with the hydrocarbon backbone and will not be interpreted here.

Contact Angle Measurements. Table 3 lists the contact angle values measured for several probe liquids on the surfaces of the cyclopropyl-terminated SAMs. Figure 7 also plots the contact angle data collected for the SAMs having the longest even ($n = 12$; Figure 7a) and odd ($n = 13$; Figure 7b) chain lengths. For comparison, we chose to examine vinyl- and isopropyl-terminated SAMs in addition to the classic methyl-terminated SAMs.

Table 3. Advancing Contact Angles (deg) Measured on Cyclopropyl-, Methyl-, Isopropyl-, and Vinyl-Terminated SAMs using Various Probe Liquids; Values of Hysteresis (Difference between Advancing and Receding Contact Angles) Are Given in Parentheses

	W	F	MF	DMF	ACN	SQ	HD
CyPr 9	99 (12)	78 (9)	61 (9)	51 (8)	49 (13)	26 (14)	≤10 (−)
CyPr 10	101 (12)	80 (8)	62 (9)	53 (8)	51 (13)	29 (12)	≤10 (−)
CyPr 11	101 (11)	78 (8)	61 (9)	53 (8)	50 (12)	28 (11)	≤10 (−)
CyPr 12	103 (11)	81 (8)	64 (8)	55 (7)	51 (10)	29 (11)	≤10 (−)
CyPr 13	101 (11)	79 (8)	62 (7)	54 (6)	51 (9)	28 (10)	13 (−)
$CH_3CH_2$9	114 (11)	94 (10)	78 (8)	72 (5)	64 (8)	51 (9)	46 (8)
$CH_3CH_2$10	114 (10)	96 (8)	81 (6)	75 (5)	67 (9)	54 (7)	48 (8)
$CH_3CH_2$11	115 (10)	95 (9)	79 (9)	72 (6)	64 (8)	53 (8)	47 (8)
$CH_3CH_2$12	114 (10)	98 (8)	84 (8)	76 (7)	67 (8)	55 (8)	49 (8)
$CH_3CH_2$13	115 (10)	96 (8)	81 (10)	73 (7)	65 (8)	53 (8)	47 (7)
IPr 12	109 (10)	91 (10)	77 (9)	66 (9)	62 (8)	49 (10)	40 (8)
IPr 13	110 (10)	90 (9)	76 (9)	66 (8)	62 (9)	48 (11)	41 (7)
vinyl 12	100 (11)	83 (11)	54 (10)	45 (11)	32 (13)	35 (12)	31 (11)
vinyl 13	101 (11)	83 (11)	55 (11)	46 (10)	33 (12)	35 (12)	31 (10)

[a] The values reported here are the average of at least 12 measurements (reproducible within ±1°). Entries marked by (−) could not be recorded because the receding contact angles are <10° (commonly defined as fully wettable). Probe liquids used in this experiment are W = water, F = formamide, MF = *N*-methylformamide, DMF = *N*,*N*-dimethylformamide, ACN = acetronitrile, SQ = squalane, HD =hexadecane.

The contact angle data for all of the probe liquids demonstrate that the methyl-terminated SAMs are universally the least wettable, followed by the isopropyl-terminated SAMs. Because methyl and isopropyl groups can interact only through dispersive interactions, the trend observed merely reflects the ability of solvent molecules to interact with the surfaces through short-range attractive forces (53). Interestingly, given that interfacial methyl groups are less wettable than methylene groups (31, 33), one might have predicted that the wettability would decrease upon substituting a single CH_3 group in a normal alkanethiolate SAM with two CH_3 groups. The fact that the opposite trend is observed can be interpreted in the context of the model proposed by Shon et al., which relates interfacial wettability to the density of atomic contacts per unit area of a surface in contact with a probe liquid (25). When applied to the present system and with the knowledge that the lattice spacing of the terminal groups in methyl-terminated and isopropyl-terminated SAMs is the same (52), the Shon et al. model would predict a greater density of atomic contacts for isopropyl surfaces than for methyl surfaces, and thus enhanced wettability for the former surfaces, which is consistent with the experimental observations reported here. Nevertheless, it is also possible that enhanced solvent intercalation (54) might be respon-

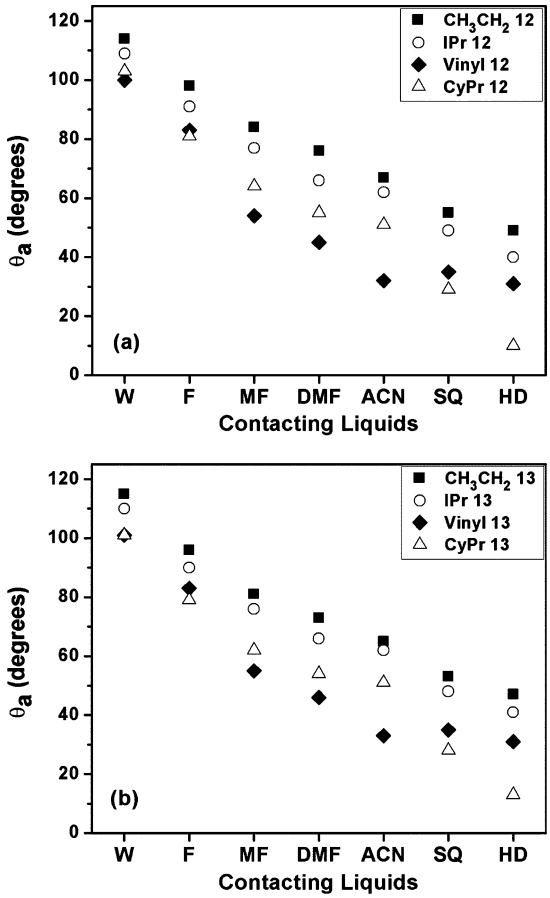

FIGURE 7. Comparison of the contact angles using various probe liquids for methyl- (■), isopropyl- (○), vinyl- (◆), and cyclopropyl-terminated SAMs (△) of (a) the even (n = 12) and (b) odd chains (n = 13). The probe liquids are W = water, F = formamide, MF = *N*-methylformamide, DMF = *N*,*N*-dimethylformamide, ACN = acetronitrile, SQ = squalane, HD = hexadecane (see also Table 3).

sible for (or at least contribute to) the enhanced wettability of the isopropyl-terminated SAMs.

Figure 7 shows further that the vinyl- and cyclopropyl-terminated SAMs are markedly more wettable than the two previous systems. According to the analysis given above, the enhanced wettability of these surfaces might arise from either intercalation effects or an increased density of atomic contacts between the interfaces and the contacting liquids. We note, however, that the vinyl-terminated SAMs expose π bonds at the interface; similarly, the bent bonds (i.e., banana-shaped orbitals) of the cyclopropyl ring have intermediate character between σ and π (55). It is also plausible that the enhanced wettability of these two films arises from the greater polarizability of their π-type terminal groups.

There are, however, differences in wettability between these two latter systems that warrant further discussion (see Figure 7). For the nonpolar contacting liquids (squalane and hexadecane), the fact that the cyclopropyl-terminated films are more wettable than the vinyl-terminated films can be rationalized by the Shon et al. model (25), where the cyclopropyl terminus offers a greater density of atomic contacts compared to the vinyl-terminated films. For the polar contacting liquids (save for water and formamide, which possess the greatest surface tensions and are thus less

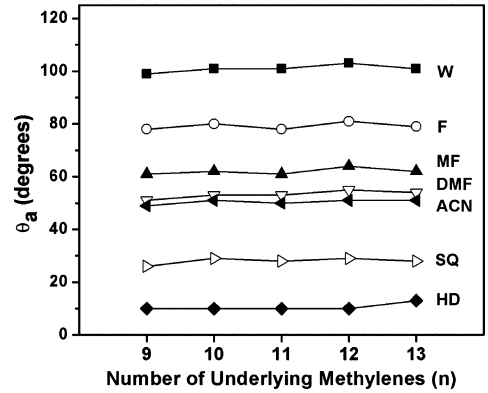

FIGURE 8. Contact angle data of cyclopropyl-terminated SAMs with respect to chain length using various probe liquids (W = water, F = formamide, MF = *N*-methylformamide, DMF = *N*,*N*-dimethylformamide, ACN = acetronitrile, SQ = squalane, HD = hexadecane; see also Table 3).

easily influenced by small variations in interfacial structure/composition), the trend is reversed. The enhanced wettability of the vinyl-terminated films by methylformamide, dimethylformamide, and acetonitrile can be rationalized on the basis of their strong dipole−induced dipole interaction with the polarizable π-bond of the vinyl group and/or by mutually attractive $\pi-\pi$ interactions between these liquids and the terminal vinyl group.

Figure 8 shows the wettability of the cyclopropyl-terminated SAMs as a function of chain length. For all contacting liquids (save for hexadecane, which completely wets the surfaces), a small but reproducible "odd−even" parity effect can be observed (29, 56, 57). Our proposed orientation of the cyclopropyl terminal group (see Figure 5) indicates that for the films having even-numbered chain lengths, the terminal group is oriented roughly normal to the surface, principally exposing the edge of the ring at the interface. In contrast, for the films having odd-numbered chain lengths, the terminal group is aligned more parallel to the surface, exposing an enhanced density of atomic contacts at the interface. As noted above and in a previous report (25), this phenomenon can be used to rationalize an enhanced wettability of the films having odd-numbered chain lengths.

Finally, based on wetting studies of polyethylene (PE) surfaces, Johnson and Dettre reported the advancing contact angle of water on PE film varies from 92° to 107° depending on the density of the polymer (58). The commonly accepted values for the advancing contact angle of water on PE films is 94°, which was obtained from a sample of PE having five methyl groups per 1000 carbon atoms in the polymer chain (59, 60). Because an increase in the number of methyl groups decreases polymer density, it is therefore plausible that a PE film having 21 methyl groups per 1000 carbon atoms in the polymer chain would exhibit a water contact angle of ∼101−105°, as has been reported (61). A similar value of 103° was reported for low-density PE films (11), and on PE deposited on glass slides (62). In contrast, nonpolar probe liquids (e.g., hexane and hexadecane) showed complete wetting of the PE surfaces (i.e., contact angle values of ∼0°) (60, 62).

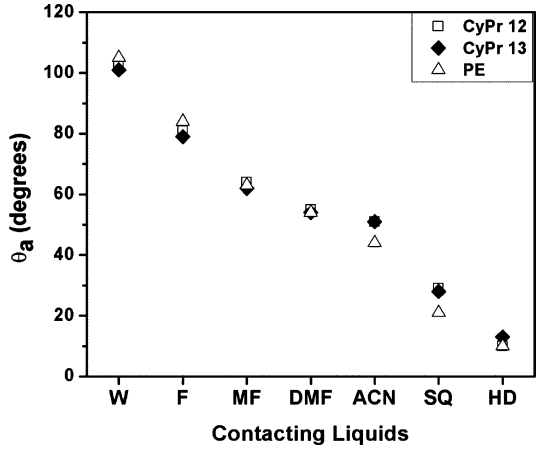

FIGURE 9. Contact angle data obtained with a wide variety of probe liquids (W = water, F = formamide, MF = *N*-methylformamide, DMF = *N*,*N*-dimethylformamide, ACN = acetronitrile, SQ = squalane, HD = hexadecane) on PE films (Δ) and on cyclopropyl-terminated SAMs having the longest even (n = 12, □) and odd chain lengths (n = 13, ◆).

To provide a more comprehensive comparison, we collected wettability data for all of the probe liquids on PE films. Figure 9 shows the contact angles of the two cyclopropyl-terminated monolayers having the longest chain lengths together with the contact angles collected on the PE films. Within experimental error (i.e., ±2°), the entire collection of probe liquids wets the SAMs and the polymer films identically. Given the broad range of probe liquids used (i.e., from polar protic to nonpolar aprotic), this comparison demonstrates that the interface of the cyclopropyl-terminated SAMs is similar in chemical structure/composition to that of PE films, suggesting that appropriately designed SAMs can serve as ideal models of polymeric interfaces without complications arising from surface reconstruction. Although cross-linking can be used to limit recronstruction in polymer films, the cross-links themselves can influence the interfacial properties. SAMs thus offer a convenient model system for evaluating these effects.

CONCLUSIONS

The adsorption of ω-cyclopropylalkanethiols on gold afforded densely packed and well-ordered monolayer films. The structure of the new films was evaluated by using ellipsometry and PM-IRRAS, and their interfacial properties were evaluated using contact angle goniometry. Both ellipsometry and PM-IRRAS data are consistent with the C−C bond of the three-membered ring opposite to the alkyl chain lying parallel to the surface. The orientation of the cyclopropyl groups with respect to the surface normal varied systematically with the number of methylene groups in the chain of the adsorbate molecule (i.e., odd vs even). Although only small variations in the wettability of the surfaces were found, these variations were present for all types of contacting liquids used. Furthermore, comparison of the wettabilities of cyclopropyl-, methyl-, vinyl-, and isopropyl-terminated SAMs revealed that the contact angle values depended on the density of atomic contacts at the interface of the films. Additional differences in the wettabilities of vinyl- and cyclopropyl-terminated SAMs were attributed to π−π interactions across the interface of the former films. Importantly, the wettability of the cyclopropyl-terminated SAMs was identical to that of PE surfaces for a wide variety of contacting liquids. The remarkable consistency of the data warrants further investigation of the use of SAMs to mimic the interfacial properties of polymeric materials.

Acknowledgment. We gratefully acknowledge support from the Robert A. Welch Foundation (E-1320) and the Texas Center for Superconductivity at the University of Houston.

Supporting Information Available: ^{1}H and ^{13}C NMR spectra of all cyclopropyl-terminated alkanethiols (PDF). This material is available free of charge via the Internet at http://pubs.acs.org.

REFERENCES AND NOTES

(1) Garbassi, F.; Morra, M.; Occhiello, E. *Polymer Surfaces: From Physics to Technology*; Wiley: New York, 1998.
(2) Lee, S. H.; Ruckenstein, E. *J. Colloid Interface Sci.* **1986**, *120*, 529.
(3) Miwa, J. A.; Rosei, F. Molecular Self-Assembly: Fundamental Concepts and Applications. In *MEMS Handbook*, 2nd ed.; Gad-el-Hak, M., Ed.; CRC Press: Boca Raton, FL, 2001.
(4) Kulkarni, S. A.; Mulla, I. S.; Vijayamohanan, K. *J. Phys.: Conf. Ser.* **2006**, *34*, 322.
(5) Brenner, D. W.; Irving, D. L.; Kingon, A. I.; Krim, J.; Padgett, C. W. *Langmuir* **2007**, *23*, 9253.
(6) Lamb, B. M.; Barrett, D. G.; Westcott, N. P.; Yousaf, M. N. *Langmuir* **2008**, *24*, 8885.
(7) Hinder, S. J.; Connell, S. D.; Davies, M. C.; Roberts, C. J.; Tendler, S. J. B.; Williams, P. M. *Langmuir* **2002**, *18*, 3151.
(8) Park, H.-H.; Jamison, A. C.; Lee, T. R. *Nanomedicine* **2007**, *2*, 425.
(9) Ishida, T. Self-Assembled Monolayers for Molecular Nanoelectronics. In *Chemistry of Nanomolecular Systems: Towards the Realization of Nanomolecular Devices*; Nakamura, T., Matsumoto, T., Tada, H., Sugiura, K., Eds.; Springer Series in Chemical Physics; Springer: New York, 2002.
(10) Onclin, S.; Ravoo, B. J.; Reinhoudt, D. N. *Angew. Chem., Int. Ed.* **2005**, *44*, 6282.
(11) Holmes-Farley, S. R.; Bain, C. D.; Whitesides, G. M. *Langmuir* **1988**, *4*, 921.
(12) Drelich, J.; Miller, J. D.; Hupka, J. *J. Colloid Interface Sci.* **1993**, *155*, 379.
(13) Chaudhury, M. K. *Mater. Sci. Eng.* **1996**, *R16*, 97.
(14) Young, T. *Miscellaneous Work of the Late Thomas Young*; Peacock, G., Ed.; Kessinger: London, 1855; Vol. 1.
(15) Owens, D. K.; Wendt, R. C. *J. Appl. Polym. Sci.* **1969**, *13*, 1741.
(16) Johnson, R. E., Jr.; Dettre, R. H. *J. Phys. Chem.* **1964**, *68*, 1744.
(17) Nuzzo, R. G.; Allara, D. L. *J. Am. Chem. Soc.* **1983**, *105*, 4481.
(18) Ulman, A. *Chem. Rev.* **1996**, *96*, 1533.
(19) Laibinis, P. E.; Whitesides, G. M.; Allara, D. L.; Tao, Y. T.; Parikh, A. N.; Nuzzo, R. G. *J. Am. Chem. Soc.* **1991**, *113*, 7152.
(20) Zisman, W. A. In *Contact Angle, Wettability, and Adhesion*; Fowkes, F. M., Ed.; Advances in Chemistry Series; American Chemical Society: Washington, D.C., 1964; Vol. 43, pp 1−51.
(21) Langmuir, I. *Science* **1938**, *87*, 493.
(22) Graupe, M.; Koini, T.; Kim, H. I.; Garg, N.; Miura, Y. F.; Takenaga, M.; Perry, S. S.; Lee, T. R. *Colloids Surf., A* **1999**, *154*, 239.
(23) Colorado, R., Jr.; Villazana, R. J.; Lee, T. R. *Langmuir* **1998**, *14*, 6337.
(24) Graupe, M.; Takenaga, M.; Koini, T.; Colorado, R., Jr.; Lee, T. R. *J. Am. Chem. Soc.* **1999**, *121*, 3222.
(25) Shon, Y.-S.; Lee, S.; Colorado, R., Jr.; Perry, S. S.; Lee, T. R. *J. Am. Chem. Soc.* **2000**, *122*, 7556.
(26) Lee, S.; Puck, A.; Graupe, M.; Colorado, R., Jr.; Shon, Y.-S.; Lee, T. R.; Perry, S. S. *Langmuir* **2001**, *17*, 7364.
(27) Miura, Y. F.; Takenaga, M.; Koini, T.; Graupe, M.; Garg, N.; Graham, R. L., Jr.; Lee, T. R. *Langmuir* **1998**, *14*, 5821.
(28) Wenzl, I.; Yam, C. M.; Barriet, D.; Lee, T. R. *Langmuir* **2003**, *19*, 10217.

(29) Sellers, H.; Ulman, A.; Shnidman, Y.; Eilers, J. E. *J. Am. Chem. Soc.* **1993**, *115*, 9389.
(30) Tao, F.; Bernasek, S. L. *Chem. Rev.* **2007**, *107*, 1408.
(31) Tao, Y.-T.; Lee, M. T.; Chang, S. C. *J. Am. Chem. Soc.* **1993**, *115*, 9547.
(32) Tao, F.; Bernasek, S. L. *Chem. Rev.* **2007**, *107*, 1408.
(33) Tao, Y. T. *J. Am. Chem. Soc.* **1993**, *115*, 4350.
(34) Mikulski, P. T.; Herman, L. A.; Harrison, J. A. *Langmuir* **2005**, *21*, 12197.
(35) March, J. *Advanced Organic Chemistry: Reactions, Mechanisms, and Structure*, 2nd ed.; McGraw-Hill: New York, 1977.
(36) Simmons, H. E.; Smith, R. D. *J. Am. Chem. Soc.* **1959**, *81*, 4256.
(37) Bain, C. D.; Troughton, E. B.; Tao, Y. T.; Evall, J.; Whitesides, G. M.; Nuzzo, R. G. *J. Am. Chem. Soc.* **1989**, *111*, 321.
(38) Laibinis, P. E.; Hickman, J. J.; Wrighton, M. S.; Whitesides, G. M. *Science* **1989**, *245*, 845.
(39) If we assume the chain tilt for both systems is the same (i.e., ~30°) and the terminal C−C bond of the methyl-terminated SAM and the shortest diagonal of the cyclopropyl ring in the cyclopropyl-terminated SAM are both aligned along the chain axis, then the projection lengths of these components in the plane normal to the surface are 1.34 Å (i.e., 1.54 × cos 30) for the methyl group vs 1.13 Å (i.e., 1.31 × cos 30) for the cyclopropyl ring.
(40) Isaacs, N. *Physical Organic Chemistry*, 2nd ed.; Addison Wesley Longman: London, 1995.
(41) Eliel, E. L.; Wilen, S. H.; Mander, L. N. *Stereochemistry of Organic Compounds*; John Wiley & Sons: New York, 1994.
(42) Wiberg, K. B. *Acc. Chem. Res.* **1996**, *29*, 229.
(43) Yamanoi, Y.; Yonezawa, T.; Shirahata, N.; Nishihara, H. *Langmuir* **2004**, *20*, 1054.
(44) Lee, J. K.; Lee, K.-B.; Kim, D. J.; Choi, I. S. *Langmuir* **2003**, *19*, 8141.
(45) Snyder, R. G.; Strauss, H. L.; Elliger, C. A. *J. Phys. Chem.* **1982**, *86*, 5145.
(46) Porter, M. D.; Bright, T. B.; Allara, D. L.; Chidsey, C. E. D. *J. Am. Chem. Soc.* **1987**, *109*, 3559.
(47) Simmons, H. E.; Blanchard, E. P., Jr.; Hartzler, H. D. *J. Org. Chem.* **1966**, *31*, 295.
(48) Socrates, G. *Infrared and Raman Characteristic Group Frequencies*; Wiley: New York, 2000.
(49) Jiang, J.; Krauss, T. D.; Brus, L. E. *J. Phys. Chem. B* **2000**, *104*, 11936.
(50) Bradshaw, A. M.; Richardson, N. V. *Pure Appl. Chem.* **1996**, *68*, 457.
(51) Lummerstorfer, T.; Hoffmann, H. *Langmuir* **2004**, *20*, 6542.
(52) Kim, H. I.; Graupe, M.; Oloba, O.; Koini, T.; Imaduddin, S.; Lee, T. R.; Perry, S. S. *Langmuir* **1999**, *15*, 3179.
(53) Fowkes, F. M. *Ind. Eng. Chem.* **1964**, *56*, 40.
(54) Timmons, C. O.; Zisman, W. A. *J. Colloid Interface Sci.* **1966**, *22*, 165.
(55) Bernett, W. A. *J. Chem. Educ.* **1967**, *44*, 17.
(56) Bain, C. D.; Whitesides, G. M. *Angew. Chem.* **1989**, *101*, 522.
(57) Whitesides, G. M.; Laibinis, P. E. *Langmuir* **1990**, *6*, 87.
(58) Johnson, R. E., Jr.; Dettre, R. H. *Surf. Colloid Sci.* **1969**, *2*, 85.
(59) Bernett, M. K.; Zisman, W. A. *J. Phys. Chem.* **1959**, *63*, 1911.
(60) Wu, S. *Polymer Interface and Adhesion*; Marcel Dekker: New York, 1982; p 138.
(61) Adam, N. K.; Elliott, G. E. P. *J. Chem. Soc.* **1962**, 2206.
(62) Shon, Y.-S.; Colorado, R., Jr.; Williams, C. T.; Bain, C. D.; Lee, T. R. *Langmuir* **2000**, *16*, 541.

AM1001585